Tomer Valency
e-mail: valency@tx.technion.ac.il

Miriam Zacksenhouse
e-mail: mermz@tx.technion.ac.il

Sensory Motor Integration Laboratory,
Faculty of Mechanical Engineering,
Technion-Israel Institute of Technology,
Haifa, Israel[1]

Accuracy/Robustness Dilemma in Impedance Control

Impedance control facilitates the execution of tasks that involve contact with the environment. However, task performance depends on the accuracy at which the desired impedance is attained. This paper focuses on feedback methods for implementing impedance control and reveals the underlying conflict between impedance accuracy and robustness to uncertainties. Furthermore, we propose a novel yet practical method that facilitates robustness while maintaining accurate impedance tracking. Eigenvalue analysis and simulation results are presented to demonstrate the accuracy/robustness dilemma and the relative merits of the different methods. [DOI: 10.1115/1.1590685]

1 Introduction

The well-known inner/outer approach to interaction control [1–5] has been developed to overcome the problems of robustness [6] and computation complexity of impedance control [7,8]. The resulting control method is indeed robust to uncertainties in the dynamic model of the robot but introduces impedance errors, which may lead to ''contact instability'' [8,9]—the same problem which impedance control has been designed to overcome.

Impedance control has been proposed by Hogan [7] as a fundamental strategy for controlling robots in constrained environments. It regulates both the force and the trajectory to endow the end-effector with dynamic properties that may be inherently different from its mechanical properties. The acquired properties may be designed to enhance the performance of the robot in contact tasks, so impedance control is especially beneficial for cooperating robots [10], robot-human cooperation [11,12], and assembly tasks [13–16]. Moreover, since impedance control is a general method, which includes both force and trajectory control as special cases, it provides a powerful yet flexible tool for planning complicated robotic tasks. However, despite its important benefits, this control strategy is not widely used.

The original impedance control method [7] depends inherently on the dynamic model of the robot and is therefore termed here the dynamics based impedance control (DB-IC). It relies on forcing the end-effector to accelerate in such a way that it appears to have the desired impedance, given the measured position, velocity, and interaction force. The required control force depends on the dynamics of the robot. Hence, this method relies inherently on an accurate model of the robot's dynamics and is very sensitive to the model's uncertainties [17,2]. Other issues concerning the DB-IC are the significant computational demands and the special structure of the control algorithm that impedes integration with existing industrial controllers.

Three approaches have been suggested to enhance the robustness of impedance control: (1) low-order impedance control strategies, (2) adaptive and robust control methods [18–21], and (3) the inner/outer control strategy [1–3]. Low-order impedance control strategies, such as stiffness control [22] and natural admittance control [23,24], do not modify the inertial component of a manipulator's impedance, and are thus less sensitive to model uncertainties. However, while these strategies might be appropriate for assembly tasks [13,16,24,25], they do not extend to general impedance control tasks like those involving human-robot or robot-robot cooperation. Adaptive [19] and robust [20] methods may be applied to reduce the sensitivity of the underlying impedance control strategy to modeling uncertainties. However, they do not modify the inherent advantages and disadvantages of the impedance control strategies, and do not contribute to their comparison. Indeed these methods may be applied to any impedance control strategy, at the expense of increased computation load.

In contrast, the inner/outer approach establishes an inherently novel impedance control strategy, which not only enhances the robustness but also facilitates integration with industrial robots[1–4,17]. In this article, we focus on the inner/outer method, and show that its robustness is achieved at the expense of accurate tracking of the desired impedance. We describe the accuracy/robustness dilemma, and proceed to propose a method that facilitates robustness while maintaining accurate impedance tracking.

The inner/outer impedance control method implements the impedance control by tracking the trajectory of the desired impedance model. The impedance model is subjected to the same interaction forces as those measured at the end-effector, but is otherwise independent of the actual position of the robot. The desired position vector is tracked using an internal position controller, so we refer to it as the position based impedance control (PB-IC). This method eliminates the inherent dependency on the dynamic model of the robot. The internal position controller may use the dynamic model of the robot but, since it includes error correction mechanisms, is less sensitive to model uncertainties. It should be noted that this method depends on the kinematic model and is sensitive to uncertainties in the kinematic parameters. However, sensitivity to kinematic uncertainties is common to all methods and is much less significant than sensitivity to dynamic uncertainties, and hence will not be discussed here.

More importantly, the PB-IC introduces impedance errors whenever the actual position of the robot differs from that of the model. Such position discrepancies often result from controller errors or external, unmeasured disturbances, which are especially important in contact tasks. Essentially, the inherent impedance of the position controller becomes significant whenever there are considerable state errors. The inherent impedance of the position controller, which is determined mainly by the gains of the inner controller, differs, in general, from the desired impedance, and thus induces impedance errors. Using adaptive or robust control methods[2,21] in the inner control loop only partly eliminates that problem, since it does not overcome external and unmeasured disturbances. The poor impedance tracking accuracy undermines the applicability of analytic planning tools and restricts the method to simple tasks in which the impedance can be planned by trial and error.

We propose a new method, which overcomes the shortcomings of both the DB-IC and the PB-IC. The proposed method is designed to take advantage of the error-correction capabilities of position controllers, like the PB-IC, while maintaining good impedance tracking performance, like the DB-IC. The method re-

[1]Fax: +972-4-829-5711

Contributed by the Dynamic Systems, Measurement, and Control Division of THE AMERICAN SOCIETY OF MECHANICAL ENGINEERS for publication in the ASME JOURNAL OF DYNAMIC SYSTEMS, MEASUREMENT, AND CONTROL. Manuscript received by the ASME Dynamic Systems and Control Division October 29, 2001; final revision, January 23, 2003. Associate Editor: Y. Chait.

sembles the PB-IC except that the desired trajectory is based on an instantaneous model, whose initial state is updated to the current state of the robot. Using the proposed approach, it is possible to trade robustness against impedance accuracy.

In Sec. 2 the DB-IC and PB-IC are mathematically formulated and qualitatively evaluated in terms of robustness and impedance accuracy. These issues are made precise in Sec. 3 using a one-dimensional linear robot. A novel method of implementation is presented in Sec. 4 and compared to the DB-IC and PB-IC methods. Two-dimensional simulations are presented in Sec. 5 to illustrate these issues in the general robotic case. The accuracy/robustness dilemma and the merits of the different methods are discussed in Sec. 6.

2 Impedance Control

2.1 Dynamic Based Impedance Control (DB-IC). The dynamics of a manipulator with n degrees of freedom can be described by [17]:

$$H(q)\ddot{q}+h(q,\dot{q})=\tau+J^{T}F_{\text{int}}, \tag{1}$$

where q is the joint displacement vector; $H(q)$ is the $n\times n$ symmetric, positive definite inertia matrix; $h(q,\dot{q})$ is the $n\times 1$ vector of the joint torque due to centrifugal, gravity, and friction forces; τ is the $n\times 1$ vector of the joint torque/force supplied by the actuators; J is the $n\times 6$ configuration-dependent Jacobian that relates the joint velocity to the end-effector velocity; and F_{int} denotes the force exerted by the environment on the end-effector.

The goal of impedance control is to endow the robot with the desired end-effector impedance, as specified by the impedance equation [7]:

$$F_{\text{int}}=K(x_0-x_r)+B(\dot{x}_0-\dot{x}_r)-M\ddot{x}_r, \tag{2}$$

where x, $\dot{x}$, $\ddot{x}$ are the position, velocity and acceleration vectors of the end-effector in the task space, and the indices $*_0$ and $*_r$ refer to the virtual and real values, respectively. The matrices K, B, M include the stiffness, damping, and inertia coefficients, respectively. The DB-IC method [7] uses forward kinematics $x=L(q)$ and the velocity transformation $\dot{x}=J\dot{q}$ to determine the current position and velocity of the end-effector from joint measurements. The control law is derived to fulfill the impedance Eq. (2) by forcing the robot to move at the required end-effector acceleration, given the current position and velocity. Thus, by using the acceleration transformation $\ddot{x}=\dot{J}\dot{q}+J\ddot{q}$ and the robot dynamic Eq. (1), the impedance control law is given by:

$$\tau_{DB\text{-}IC}=-J^{T}F_{\text{int}}+h(q,\dot{q})+H(q)J^{-1}(M^{-1}\times\{K[x_0-L(q)]+B(\dot{x}_0-J\dot{q})-F_{\text{int}}\}-\dot{J}\dot{q}). \tag{3}$$

The resulting control law requires precise knowledge of the dynamic model (Eq. (1)) and the parameter values [19]. Although adaptive methods can reduce the sensitivity to uncertainties in the model's parameters [10,19], they rely on a detailed dynamic model, and increase the computational complexity. Furthermore, the DB-IC implicitly neglects the time delays induced by the controller and by the feedback loop, so it is not appropriate when the force or position change rapidly compared to those delays.

2.2 Position Based Impedance Control (PB-IC)

2.2.1 Reference Trajectory. The DB-IC law, given by Eq. (3), depends strongly on the dynamic model of the robot. To overcome this problem, and to increase the robustness of the impedance controller to modeling uncertainties, an alternative control method was proposed in the literature. This method uses an inner position controller to track the reference trajectory of the impedance model [1–3]. The impedance model has the same form as Eq. (2) but the real values $*_r$ are replaced with the values of the desired impedance model $*_m$:

$$F_{\text{int}}=K(x_0-x_m)+B(\dot{x}_0-\dot{x}_m)-M\ddot{x}_m. \tag{4}$$

It is noted that the state of the model $*_m$ may differ from the real state of the robot $*_r$, and that this difference may hinder accurate impedance tracking, as will be discussed in Sec. 2.2.3. The impedance model is initialized to the initial position of the end-effector and modified only by the force feedback. Integrating the second order differential equation of the impedance model along the task generates the desired reference trajectory to be tracked by the inner position controller.

2.2.2 Inner Loop Position Controller. The inner loop position controller can be any stable controller. It can be a simple proportional, integral, differential (PID) controller [1,3]; possibly with dynamic compensation [17]; an adaptive controller [2], or a robust position controller. The inner loop position controller acts in the robot joint space and so requires inverse kinematics, and the inverse Jacobian, to transform the reference trajectory to the joint space, using:

$$q_d=L^{-1}(x_m);\quad \dot{q}_d=J^{-1}\dot{x}_m.$$

In order to facilitate the comparison with the DB-IC we use a PD controller with dynamic compensation. The resulting PB-IC law is:

$$\tau_{PB\text{-}IC}=-J^{T}F_{\text{int}}+h(q_r,\dot{q}_r)+H(q_r)\times[\ddot{q}_d+D_{PB}(\dot{q}_d-\dot{q}_r)+P_{PB}(q_d-q_r)], \tag{5}$$

where D_{PB} and P_{PB} are the differential and proportional gain matrices, respectively.

2.2.3 Impedance Tracking. By tracking the reference trajectory generated by the impedance model the robot behaves as having the desired impedance, and thus tracks the desired impedance. However, this correspondence fails if the position of the robot deviates from that of the reference trajectory, as may occur due to controller errors or perturbations. When deviations occur, tracking the reference trajectory would cause the robot to act as having an impedance that is different from the desired one and reflects the dynamic characteristics of the controller itself.

Indeed, the inner loop controller should be designed to drive state errors to zero, not to match the dynamics of the desired impedance. The resulting poles introduced by the inner controller (see Sec. 3.1) should be faster than those of the desired impedance model, so in normal operation they are silent. However, they become significant in response to disturbances, and cause the robot to respond as having different impedance than desired (as demonstrated in Sec. 5.4), thereby hindering accurate tracking of the desired impedance.

3 Linear One-Dimensional Analysis

The relative advantages and disadvantages of the different control laws, and in particular, the impedance error introduced by the PB-IC, are demonstrated using a linear one-dimensional robot model. Specifically, the robot model is linearized around the point of contact, and assuming that the different degrees of freedom are uncoupled, is reduced to a single degree of freedom. These simplifications facilitate the clarification of the underlying accuracy/robustness dilemma.

Important practical issues as joint friction, Coulomb friction, and sensor/actuator noncollocation were omitted from this study, as the intent is to investigate the accuracy/robustness dilemma. Furthermore, it is noted that joint friction is proportional to joint velocity, which is low in many force control applications [21]. For excellent discussions on the effect of friction on the stability of interaction controllers, see Refs. [23] and [26].

3.1 Mathematical Formulation. The dynamics of the one-dimensional manipulator, shown schematically in Fig. 1, can be described by:

$$-M_p\ddot{x}_p+B_p(\dot{x}_{0,p}-\dot{x}_p)+K_p(x_{0,p}-x_p)=F_{\text{int}}+U_{controller}, \tag{6}$$

Table 1 Nominal values of the second pair of eigenvalues for each of the impedance control methods. The eigenvalues are expressed as natural frequency and damping ratio $\lambda_{0_{1,2}} = -\omega_0\zeta_0 \pm j\omega_0\sqrt{1-\zeta_0^2}$.

Method	Closed loop ζ_0	Closed loop ω_0^2
DB-IC	ζ_m	ω_m^2
PB-IC	$\frac{1}{2}\frac{D_{PB}}{\sqrt{P_{PB}}}$	P_{PB}
IM-IC	$\sqrt{1+\Delta t(D_{IM}-2\zeta_m\omega_m)}\left[\zeta_m+\frac{(P_{IM}-\omega_m^2)\Delta t}{2\omega_m(1+\Delta t(D_{IM}-2\zeta_m\omega_m)}\right]$ $=\frac{\omega_0}{\omega_m}\zeta_m+\frac{P_{IM}-\omega_m^2}{2\omega_0^2}\omega_0\Delta t$	$\omega_m^2[1+\Delta t(D_{IM}-2\zeta_m\omega_m)]$

where the index $*_p$ refers to the state of the manipulator plant, $*_{0,p}$ its virtual state; K_p and B_p are the stiffness and damping coefficients of the manipulator, respectively, as seen by the environment; M_p is the manipulator mass; and $U_{controller}$ is the controller force. For the sake of simplicity the one-dimensional analysis is conducted for the case when the interaction force is state independent, as may occur when the interaction force is externally controlled by a human or other mechanism. As detailed below (see also the Appendix) the impedance model in this case is decoupled from the dynamics of the controlled manipulator.

The one-dimensional presentation of the robot's dynamics in Eq. (6) is derived directly from the general model of Eq. (1) and described in terms of the physical parameters of intertia, damping and stiffness. To facilitate stability analysis, it may be expressed as a general second-order system using the damping ratio $\zeta = \frac{1}{2}B/\sqrt{KM}$, natural frequency $\omega = \sqrt{K/M}$, and static gain $G = 1/M$, as:

$$-\ddot{x}_p - 2\zeta_p\omega_p\dot{x}_p - \omega_p^2 x_p = (F_{\text{int}} + U_{controller})G_p. \tag{7}$$

Given the manipulator's dynamics in Eq. (6), the one-dimensional impedance model Eq. (4) and the control laws Eqs. (3) and (5), the corresponding control forces $U_{DB\text{-}IC}$ and $U_{PB\text{-}IC}$, for the dynamic-based and position-based control methods, respectively, are:

$$\begin{aligned} U_{DB\text{-}IC} &= -\hat{K}_p x_p - \hat{B}_p\dot{x}_p - \frac{\hat{M}_p}{M_m}[K_m(x_0 - x_p) \\ &\quad + B_m(\dot{x}_0 - \dot{x}_p) - F_{\text{int}}] - F_{\text{int}}, \\ U_{PB\text{-}IC} &= -\hat{K}_p x_p - \hat{B}_p\dot{x}_p - \hat{M}_p \\ &\quad \times[\ddot{x}_m + D_{PB}(\dot{x}_m - \dot{x}_p) + P_{PB}(x_m - x_p)] - F_{\text{int}}, \end{aligned} \tag{8}$$

where $\hat{K}_p$, $\hat{B}_p$, $\hat{M}_p$ are the estimated parameters—stiffness, damping, and mass—of the plant, and K_m, B_m, M_m are the parameters of the desired impedance. Each of the equations in Eq. (8) along with the one-dimensional impedance model in Eq. (4), forms a four-dimensional feedback system with a state vector $X = [x_m\ x_p\ \dot{x}_m\ \dot{x}_p]^T$ and an input vector $V = [x_0\ \dot{x}_0\ F_{\text{int}}]^T$. The resulting closed-loop system can be represented in the state space by $\dot{X} = AX + BV$, where the matrices A and B are given in the Appendix (Eqs. (32–35)). The eigenvalues of matrix A specify the roots of the system and thus its dynamics. One pair of eigenvalues describes the dynamics of the impedance model that does not depend on the control low, and is given by:

$$\lambda_m = -\zeta_m\omega_m \pm \omega_m\sqrt{\zeta_m^2 - 1}. \tag{9}$$

The second pair of eigenvalues describes the dynamics introduced by the plant dynamic and the specific impedance controller, and will be denoted by $\lambda_{DB\text{-}IC}$, and $\lambda_{PB\text{-}IC}$, respectively.

In the nominal case, with an accurate dynamic model (Eqs. (6) or (7)), the eigenvalues induced by the DB-IC coincide with those of the model, so: $\lambda_{DB\text{-}IC} = \lambda_m$, and there are two poles at each location. However, modeling errors would cause the roots of the feedback system to drift away from their desired location, and may lead to instability, as detailed in Sec. 3.3 below [27,28].

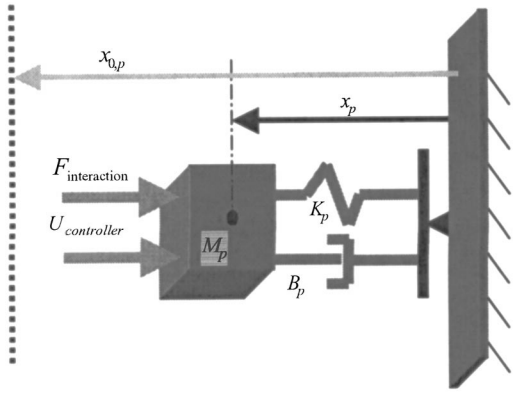

Fig. 1 One-dimensional model of a manipulator plant. The manipulator is located at x_p and characterized by mass M_p, damping B_p and stiffness K_p, as seen from the environment. The virtual position of the manipulator $x_{o,p}$ reflects the position of the manipulator when the spring is free. The manipulator is subjected to the interaction force F_{int} and the controller force $U_{controller}$.

The eigenvalues induced by the PB-IC are determined mainly by the gains of the inner controller. The dynamic compensation used here ensures that in the nominal case the eigenvalues do not depend on the parameters of the manipulator or the impedance model, and are given by:

$$\lambda_{PB\text{-}IC} = -\frac{1}{2}D_{PB} \pm \frac{1}{2}\sqrt{D_{PB}^2 - 4P_{PB}}. \tag{10}$$

Table 1 describes the nominal eigenvalues in terms of the damping ratio and the natural frequency.

3.2 Impedance Tracking. In the one-dimensional linear case, it is straightforward to select the gains of the inner PD controller so that the eigenvalues introduced by the controller in Eq. (10) coincide with the desired eigenvalues of the model ($D_{PB} = 2\zeta_m\omega_m$ and $P_{PB} = \omega_m^2$). However, in other cases, where multi-dimensional nonlinear robots are controlled, gain selection is more complicated. Furthermore, the main goal of the inner position controller is to provide good position tracking, which requires placing the associated eigenvalues appropriately. In particular, the PD gains of the position controller are usually selected such that the damping coefficient $\zeta_{PD} = 0.7$, and the natural frequency $\omega_{PD} = 4.6(\zeta_{PD}t_s)^{-1}$ [29], where t_s, the settling time, is a design parameter. The settling time is usually required to be short, so the

Table 2 Influence of model uncertainties on the eigenvalues of the controlled system, as function of the damping ratio and natural frequency of the nominal systems. The $*_p$ parameters denote the actual values and the $\hat{*}_p$ parameters denote the estimated values.

Model uncertainties	Closed loop ζ	Closed loop ω^2
$\varepsilon_M=\dfrac{\hat{M}_p-M_p}{M_p}\neq 0$	$\sqrt{(1+\varepsilon_M)}\zeta_0$	$(1+\varepsilon_M)\omega_0^2$
$\varepsilon_B=\dfrac{\hat{B}_p-B_p}{B_p}\neq 0$	$\left(1-\dfrac{\zeta_p\omega_p}{\zeta_0\omega_0}\varepsilon_B\right)\zeta_0$	ω_0^2
$\varepsilon_K=\dfrac{\hat{K}_p-K_p}{K_p}\neq 0$	$\dfrac{1}{\sqrt{1-\dfrac{\omega_p^2}{\omega_0^2}\varepsilon_K}}\zeta_0$	$\left(1-\dfrac{\omega_p^2}{\omega_0^2}\varepsilon_K\right)\omega_0^2$

resulting natural frequency is high. The above requirements place the eigenvalues in a specific region of the imaginary space, which differs, in general, from the region where the eigenvalues of the impedance model are placed. Thus, the requirements of the inner position controller may conflict with the desired impedance properties.

3.3 Controller Robustness. The sensitivities of the controlled system to errors in the estimated inertia, damping, and stiffness parameters of the model are summarized in Table 2. Each estimation error ε is expressed as the fraction of the difference between the actual $*_p$ and estimated $\hat{*}_p$ values with respect to the actual value (left column). It is noted that the effects of the estimation errors depend on the control method only through the nominal values of the natural frequency and the damping ratio. In terms of these parameters, which depend on the particular control method, the sensitivities to the estimation errors are the same, regardless of the control method.

The controlled robot is stable as long as the damping ratio ζ of the closed-loop controlled system is positive. The range of parameter uncertainties that may be tolerated without destabilizing the system determines the robustness of the system. The effect of errors in the inertia parameter is independent of the nominal position of the eigenvalues and thus is independent of the control method. By contrast, the effect of errors in either the damping or stiffness parameters depends on the nominal value of the natural frequency (and the damping ratio, in the case of damping errors), and thus on the control method. In particular, the higher the nominal natural frequency the more robust the system is.

3.4 Accuracy/Robustness Dilemma. The sensitivity to errors in the damping and stiffness parameters depends inversely on the magnitude of the nominal natural frequency ω_0, as indicated by the last two rows of Table 2 (the inverse relationship in the case of an error in the stiffness parameter becomes evident when considering the limit of small errors in which $\zeta\approx(1+(\omega_p^2/2\omega_0^2)\varepsilon_k)\zeta_0$). In the DB-IC, the desired impedance model determines the nominal natural frequency so $\omega_0=\omega_m$ (Table 1). Thus, the sensitivity to errors in the damping or stiffness parameters depends on the desired impedance. In particular, when the desired impedance is designed to have a low natural frequency in order to avoid contact instability, the resulting sensitivity is high. In the extreme case, when the error is large compared with the ratio between the dynamic properties of the plant and those of the desired impedance model, the system becomes unstable.

The PB-IC has been designed to overcome this problem and to reduce the sensitivity of the controlled system to errors in the parameters of the plant. This is accomplished by increasing the nominal natural frequency, as typical for good position controllers. As is evident from Table 2, a higher natural frequency can ensure stability under a wider range of parameter errors. However, as the natural frequency is increased, the position of the eigenvalues increasingly drifts, thereby impeding the ability of the system to accurately track the desired impedance. Thus, robustness is achieved at the expense of accurate impedance tracking—demonstrating the inherent accuracy/robustness dilemma of impedance control.

3.5 Example. As an example, consider the task of controlling a robot (plant) described by:

$$\zeta_{\mathrm{p}}=4.3205;\quad \omega_{\mathrm{p}}=21.6025\left[\frac{1}{\mathrm{s}}\right];\quad G_p=\frac{1}{7.5}\left[\frac{1}{\mathrm{kg}}\right] \tag{11}$$

to act as having the following impedance:

$$\zeta_{\mathrm{m}}=0.5401;\quad \omega_{\mathrm{m}}=10.8012\left[\frac{1}{\mathrm{s}}\right];\quad G_m=\frac{1}{30}\left[\frac{1}{\mathrm{kg}}\right]. \tag{12}$$

The task described above illustrates a situation in which a plant is forced to act with four times lower damping and four times higher inertia, and serves to illustrate the robustness/accuracy dilemma.

The PB-IC is designed to have the following parameters:

$$\begin{gathered} dt=0.01\ [\mathrm{s}];\quad t_s=10dt=0.1\ [\mathrm{s}];\quad \zeta_{PD}=0.7;\\ \omega_{PD}=4.6/(\zeta_{PD}t_s)\left[\frac{1}{\mathrm{s}}\right],\\ P_{PB}=\omega_{PD}^2=4318\left[\frac{1}{\mathrm{s}^2}\right];\quad D_{PB}=2\zeta\sqrt{P_{PB}}=92\left[\frac{1}{\mathrm{s}}\right]. \end{gathered} \tag{13}$$

In the nominal case, the eigenvalues are located at:

$$\lambda_{DB\text{-}IC}=-5.83\pm 9.1i, \tag{14}$$

$$\lambda_{PB\text{-}IC}=-46\pm 46.9i. \tag{15}$$

The eigenvalues of the DB-IC coincide with the eigenvalues of the desired impedance model. However, the eigenvalues of the PB-IC are located to the left of the desired eigenvalues. Moving the eigenvalues to the left increases the stability of the PB-IC and thus its robustness, as compared with the DB-IC. Figure 2 demonstrates the effect of errors in the coefficient of damping on the location of the eigenvalues of the DB-IC and PB-IC. It is evident that the PB-IC maintains stability over a wider range of damping errors and that the DB-IC becomes unstable at smaller error levels.

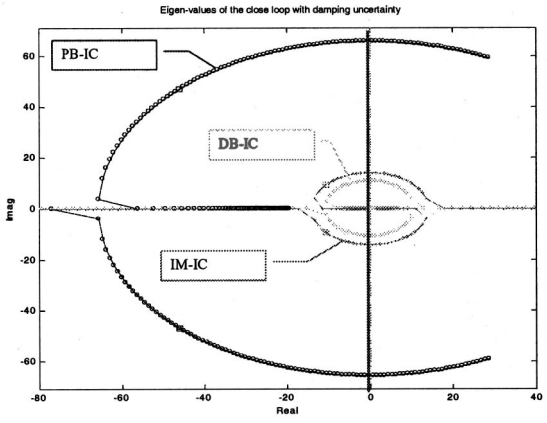

Fig. 2 Eigenvalue analysis: The effect of an error in estimating the plant damping parameter on the location of the eigenvalues of the closed-loop system, for the DB-IC, PB-IC, and IM-IC. The nominal eigenvalues are marked by squares. The relative error is varied between [−0.8,+0.8] of the real value.

4 Instantaneous Model Impedance Control (IM-IC)

The proposed method for implementing impedance control is designed to take advantage of the error-correction capabilities of position controllers, such as the PB-IC, while maintaining good impedance tracking performance, like the DB-IC. Moreover, the proposed method facilitates the trade-off between accurate impedance tracking and robust performance.

4.1 Principle of Operation. The proposed instantaneous model impedance control (IM-IC) combines the dynamic-based and position-based impedance control methods. It calculates the acceleration needed to fulfill the impedance relationship as in the DB-IC approach. Using the acceleration and the current position and velocity, it predicts the position of an instantaneous model of the desired impedance in the next time step. The predicted position is converted to the joint space and used as a reference to the inner position controller. The inner controller can be any position controller that assures stable trajectory tracking. In this work, a proportional-differential (PD) plus inverse dynamics controller is used for direct comparison with the previously described impedance control methods. The method is described by a block diagram in Fig. 3, and is unique in the use of the current state in computing the desired trajectory in the external loop, as further detailed below.

The desired trajectory is computed by integrating the impedance model in the task space for a small integration step (Δt). However, instead of integrating from the current position of the model as in PB-IC, the integration is re-initialized to the current position of the robot. This initialization corresponds to having an instantaneous impedance model, which is sensitive to the actual position of the robot, instead of a position independent impedance model as in the PB-IC [1,2,30]. Specifically, the initial state of the instantaneous model is computed from the measured joint-space position and velocity of the robot using forward kinematics and the Jacobian matrix. The impedance model is integrated from that initial state to predict its state in the next time step. Finally, the predicted task-space state is transformed back to the joint space, using inverse kinematics and the Jacobian matrix, to provide a reference signal for the inner-loop position controller.

4.2 Mathematical Formulation. Let the index $*_{im}$ denote the variables of the instantaneous impedance model. The instantaneous impedance model is initialized at each time step to the current state of the end-effector, which is computed from the joint measurements using forward kinematics: $x_{im}(t)=L[q_r(t)]$; $\dot{x}_{im}(t)=J\dot{q}_r(t)$. The instantaneous impedance model, given by

$$F_{\text{int}}=K_m(x_0-x_{im})+B_m(\dot{x}_0-\dot{x}_{im})-M_m\ddot{x}_{im}, \tag{16}$$

is integrated using the above initial conditions to predict the desired velocity in the next time step $t+\Delta t$, so

$$\dot{x}_{im}(t+\Delta t)=\dot{x}_{im}(t)+\int_t^{t+\Delta t} M_m^{-1}\{-F_{\text{int}}+B_m[\dot{x}_0(t)-\dot{x}_{im}(\tau)] + K_m[x_0(t)-x_{im}(\tau)]\}d\tau. \tag{17}$$

The integration step Δt is a design parameter. Investigation of its effect on the performance of the IM-IC is beyond the scope of this paper. However, we note that as the gradient of the required acceleration increases, a finer integration step should be used. Hence, it is recommended that the integration step be as short as is physically reasonable, and, in particular, identical to the control cycle time dt.

Similarly, the desired position is computed by double integration. If the inner control loop requires the desired acceleration, it can be isolated from the impedance model in Eq. (16) with the new values of position and velocity,

$$\ddot{x}_{im}(t+\Delta t)=M_m^{-1}\{-F_{\text{int}}(t)+B_m[\dot{x}_0-\dot{x}_{im}(t+\Delta t)] + K_m[x_0-x_{im}(t+\Delta t)]\}. \tag{18}$$

The desired position, velocity, and acceleration are transformed to the joint space using inverse kinematics $L^{-1}(\cdot)$, the inverse Jacobian matrix J^{-1}, and the derivative of the Jacobian:

$$\begin{aligned} q_d&=L^{-1}[x_{im}(t+\Delta t)],\\ \dot{q}_d&=J^{-1}\dot{x}_{im}(t+\Delta t),\\ \ddot{q}_d&=J^{-1}[\ddot{x}_{im}(t+\Delta t)-\dot{J}\dot{q}_d], \end{aligned} \tag{19}$$

where the index $*_d$ denotes the desired variables that are sent to the inner controller. Both the inverse Jacobian and its derivative, which are required to compute the desired joint space position vector in Eq. (19), are functions of the desired joint-space position and velocity. Finally, the position controller in the inner control loop generates the control force to achieve the desired position vector. In the present work, we use a proportional differential controller with dynamic compensation, so a model of the robot's dynamics (Eq. (1)) is required. The control algorithm compensates for the robot's dynamics, and adds a correction force proportional to position and velocity errors:

$$\tau_{IM\text{-}IC}=-J^TF_{\text{int}}+h(q_r,\dot{q}_r)+H(q_r)[\ddot{q}_d+D_{IM}(\dot{q}_d-\dot{q}_r) + P_{IM}(q_d-q_r)]. \tag{20}$$

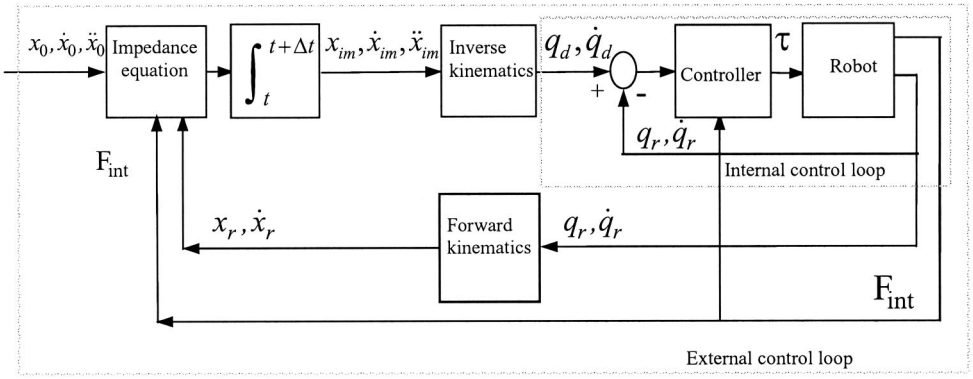

Fig. 3 Block diagram of the instantaneous model impedance control (IM-IC). See text for notation. The external state feedback, which uses the current state to compute the desired trajectory, is unique to the IM-IC.

It is noted that the position controller in the inner control loop may not require the entire desired position vector. This is advantageous when the above transformations are not available (as in robots with singular Jacobian matrix).

The primary advantage of the proposed method is in achieving good impedance accuracy while providing robustness to model uncertainties. Using the instantaneous impedance model ensures that the desired impedance relationship is maintained in the actual position of the robot, instead of the predicted position, as in the PB-IC approach. Using the inner position controller provides error correction mechanisms that increase the robustness of the controller. Furthermore, by tuning the control parameters it is possible to establish a trade-off between impedance accuracy and robustness. In the extreme case, when the integration step is zero, the IM-IC converges to the original DB-IC.

4.3 Linear One-Dimensional Analysis. As in Sec. 3, the IM-IC of a one-dimensional linear robot is analyzed to characterize its performance in terms of accuracy and robustness. Given the manipulator's dynamics in Eq. (6), the one-dimensional impedance model in Eq. (16) and the control law in Eq. (20), the corresponding control force $U_{IM\text{-}IC}$ is

$$U_{IM\text{-}IC}=-\hat{K}_p x_p-\hat{B}_p\dot{x}_p-\hat{M}_p[\ddot{x}_{im}+D_{IM}(\dot{x}_{im}-\dot{x}_p)+P_{IM}(x_{im}-x_p)]-F_{\text{int}}. \tag{21}$$

The resulting four-dimensional feedback system, given by Eqs. (21) and (16), is represented by the matrices given in the Appendix (Eqs. (36) and (37)). The two eigenvalues that represent the dynamics of the controlled system depend, in the nominal error-free case, on the gains of the inner controller, the parameters of the model, and the integration step Δt:

$$\lambda_{IM\text{-}IC}=-\omega_m\zeta_m[1+(D_{IM}-2\omega_m\zeta_m)\Delta t]-(P_{IM}-\omega_m^2)\Delta t/2 \pm\sqrt{\{\omega_m\zeta_m[1+(D_{IM}-2\omega_m\zeta_m)\Delta t]+(P_{IM}-\omega_m^2)\Delta t/2\}^2-1}. \tag{22}$$

The corresponding damping ratio and natural frequency are specified in the last row of Table 1. By controlling the gains of the inner loop controller (i.e., $D_{IM}=2\omega_m\zeta_m$, $P_{IM}=\omega_m^2$), or the integration step (i.e., $\Delta t=0$) it is possible to drive the system to behave like the impedance model.

The effects of modeling errors, expressed in terms of the nominal natural frequency and the damping ratio, are the same as in the previous two methods (Table 2). As in the PB-IC, the eigenvalues may be manipulated to increase robustness at the expense of the accuracy of impedance tracking. Specifically, the gains may be tuned to increase the natural frequency beyond the natural frequency of the impedance model, and thus to increase the robustness. Thereby, it is possible to trade off the accuracy of impedance tracking against the robustness to uncertainties. Section 5.2 explains how the IM-IC facilitates this trade-off in the general robotic case.

For the task described in Sec. 3.5, the IM-IC is designed to have the following parameters:

$$P_{im}=13.0\left[\frac{1}{\text{s}^2}\right],\qquad D_{im}=87.0\left[\frac{1}{\text{s}}\right], \tag{23}$$

and the nominal eigenvalues of the IM-IC are located at

$$\lambda_{IM\text{-}IC}=-10.1\pm 9.8i. \tag{24}$$

The eigenvalues of the IM-IC are located between the eigenvalues of the DB-IC, and the eigenvalues of the PB-IC. In this particular example, the IM-IC parameters were selected to achieve higher impedance tracking accuracy at the expense of robustness, so the eigenvalues are located closer to those of the DB-IC. Figure 2 demonstrates that the relationships between the eigenvalues are maintained when considering the effect of errors in the damping coefficient. It should be noted again that by selecting different control parameters it is possible to vary the location of the eigenvalues to increase either robustness or impedance accuracy.

5 Two-Dimensional Simulations

A two-dimensional planar robot is simulated to demonstrate how the accuracy/robustness dilemma and the insights gained from the one-dimensional analysis are manifested in the general robotic case. It is noted that both the DB-IC robustness problem and the PB-IC impedance error become more severe in the multidimensional robot case. The robustness problem is adversely affected by the higher estimation errors associated with the increasingly complex dynamic model of multidimensional robots. The impedance accuracy deteriorates in the multidimensional robot case since the gains of the internal controller in the PB-IC are selected empirically based on their trajectory tracking instead of impedance tracking capabilities.

5.1 Robotic Task. To demonstrate the contact stability [9] achieved by the different control methods, we consider a simple task, which involves contact with a rigid wall. The task includes five stages: (1) approaching a rigid wall, (2) making contact with the wall, (3) moving along a section of the wall while maintaining contact, (4) detaching from the wall, and (5) returning to the initial position. For simplification, the task is planar and the robot has two links, as shown in Fig. 4. The planar robot (bold line) should follow the desired/virtual path (dashed line), which includes contact with a rigid wall. The task is similar to the one described by Hogan [8], but involves a simpler path, which is easier to plan yet more challenging to follow.

The rigid wall is modeled as an ideal spring with constant stiffness (K_e), so the interaction force depends on the position of the manipulator. In particular, when the robot is "inside" (to the right of) the wall, the interaction force is proportional to the distance between the original position of the wall surface and the position of the robot, with the proportionality constant K_e. In contrast, when the robot is outside (to the left of) the wall there is no interaction force between the robot and the wall. Thus, the interaction force in the subsequent figures (Figs. 6–9) is directly apparent from the position of the manipulator relative to the wall.

The virtual trajectory $[x_0(t),\dot{x}_0(t)]$ is simply defined, as shown in Fig. 4. Along the x axis, the trajectory is composed of two

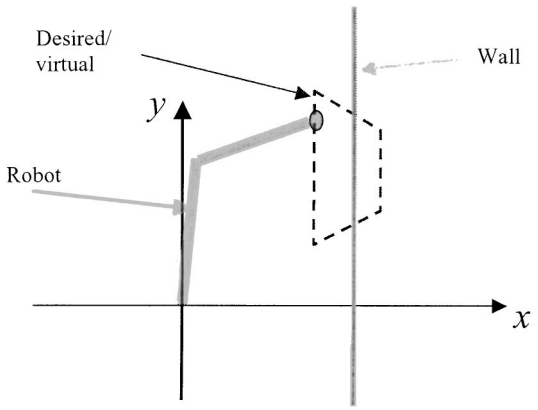

Fig. 4 Planar robotic task: The planar robot (bold line) should follow the desired/virtual path (dashed line), which includes contact with a rigid wall. The rigid wall is modeled as an ideal spring with constant stiffness (K_e), so the contact force is proportional to the extent the robot is behind (to the right of) the wall times the stiffness. When the robot is in front (to the left of) the wall it loses contact with the wall and there is no interaction force.

positions, one outside (to the left of) and one inside (to the right of) the wall, each of which is maintained for half the motion cycle. Along the *y* axis, the virtual trajectory moves up and down at a constant velocity.

Simulation parameters. The links of the robot are described by

$$l_1=40\ [\text{cm}];\quad l_2=30\ [\text{cm}];\quad m_1=8\ [\text{kg}];$$
$$m_2=5\ [\text{kg}];\quad m_{end}=4\ [\text{kg}]. \tag{25}$$

The stiffness of the contact with the wall is $K_e=10^5\,[\text{N/m}]$. The equation describing the desired impedance is given by

$$\begin{bmatrix}100 & 0\\ 0 & 100\end{bmatrix}\begin{bmatrix}\ddot{x}\\ \ddot{y}\end{bmatrix}+\begin{bmatrix}3500 & 0\\ 0 & 3500\end{bmatrix}\begin{bmatrix}\dot{x}\\ \dot{y}\end{bmatrix}+\begin{bmatrix}62{,}500 & 0\\ 0 & 62{,}500\end{bmatrix}\begin{bmatrix}x\\ y\end{bmatrix}=\begin{bmatrix}F_1\\ F_2\end{bmatrix}. \tag{26}$$

The desired impedance model is designed to successfully perform the above task with different values of wall stiffness, as shown in Fig. 5 for the nominal wall stiffness. As desired, the model contacts the wall and quickly stabilizes on the desired contact force without losing contact with the wall.

In Secs. 5.3 and 5.4, we present simulation results with the different impedance controllers in two scenarios: (1) load uncertainties and (2) excessive wall stiffness. These scenarios are designed to demonstrate the robustness/accuracy dilemma presented by the dynamic- and position-based impedance controllers. The first scenario demonstrates the sensitivity of the DB-IC to parameter uncertainties. The second scenario demonstrates the contact instability evoked by the PB-IC when the position of the robot deviates from that of the impedance model. The performance of the proposed IM-IC method is tested in the same scenarios to demonstrate its ability to overcome these difficulties.

5.2 Controller Tuning. In the one-dimensional case, the control gains of the PB-IC or the IM-IC can be computed analytically to achieve a specific dynamic behavior (see Sec. 3.2). However, in the multidimensional nonlinear robotic task the control gains are tuned to minimize position errors. In particular, the inner controller in the PB-IC is tuned based on its performance in trajectory tracking, which, in general, requires different gains than those matching the desired impedance.

In contrast, the inner controller in the IM-IC is tuned based on its performance in tracking the position of the instantaneous impedance model. In this method, close tracking of the instantaneous impedance model implies close tracking of the desired impedance. Thus, the proposed method facilitates the visualization of the impedance error as a trajectory error and guides the selection of gains that achieve good impedance tracking. Furthermore, the expected levels of uncertainties in the parameters of the dynamic model may be integrated into the tuning process to achieve the desired trade-off between robustness and accuracy.

Given the task described in Sec. 5.1, the control parameters of the PB-IC and IM-IC were tuned empirically to minimize the trajectory error with respect to the impedance model or the instantaneous impedance model, respectively. The tuning process was performed with respect to the above task and the nominal wall stiffness. The resulting proportional and differential gains that were used in the simulations are

$$P_{PB\text{-}IC}=\begin{bmatrix}150 & 0\\ 0 & 170\end{bmatrix};\quad D_{PB\text{-}IC}=\begin{bmatrix}18 & 0\\ 0 & 10\end{bmatrix},$$
$$P_{IM\text{-}IC}=\begin{bmatrix}0.5 & 0\\ 0 & 0.5\end{bmatrix};\quad D_{IM\text{-}IC}=\begin{bmatrix}0.1 & 0\\ 0 & 0.1\end{bmatrix}. \tag{27}$$

5.3 Load Uncertainties. Figures 6 and 7 depict the performance of the IM-IC and DB-IC when the actual load m_L is double the estimated load $\hat{m}_L$ ($m_{Ld}=2\hat{m}_L=8\,[\text{kg}]$). Load uncertainties are common, but we note that their effect is not mild.

Naturally, there is no effect on the behavior of the impedance model, since the desired impedance is the same. Figure 6 demonstrates that the IM-IC successfully controls the robot and the effect on its performance is not severe. However, the DB-IC causes the robot to temporarily lose its initial contact, as shown in Fig. 7. The poor performance is attributed to the insufficient compensation forces that are generated by the impedance controller as it tries to accelerate a larger than expected load. The undercompensated dynamics of the robot leads to unexpected interaction forces, which results in temporary loss of contact.

The ability of the IM-IC to perform well despite model uncertainties, as demonstrated in Fig. 6, stems from its error correction capabilities that alleviate its dependency on the dynamic model. Moreover, as mentioned in Sec. 4, the gains in the inner controller can be tuned to trade robustness off against impedance accuracy.

5.4 Excessive Stiffness. Figures 8 and 9 depict the performance of the PB-IC and the IM-IC upon contacting a wall that is twice as stiff as estimated ($K_e=2\hat{K}_e=2\times10^5\,[\text{N/m}]$ where K_e and $\hat{K}_e$ are the real and estimated values wall stiffness, respectively). The effect on the performance of the impedance model is negligible, so we should expect that with good impedance control the robot should perform well. However, the performance of the

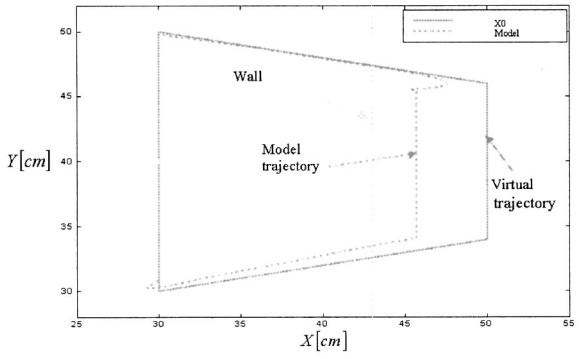

Fig. 5 Model trajectory: the model trajectory (dashed line) traced by a robot that responds according to the desired impedance model and follows the virtual trajectory (solid line) specified by the task of Fig. 4.

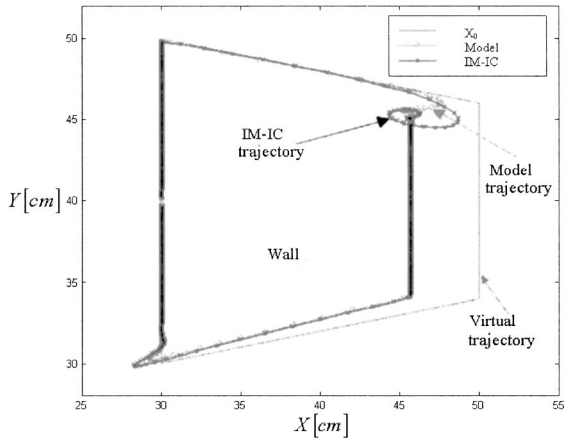

Fig. 6 The IM-IC adequately controls the robot to perform the task of Fig. 4 with a double than estimated load. The trajectory of the robot with a double than estimated load under the IM-IC (marked with x) slightly deviates from the model trajectory (marked with circles) upon hitting the wall, and the robot maintains contact.

PB-IC is severely affected, as shown in Fig. 9. Upon making contact with the wall, the robot starts to oscillate, alternately making and breaking contact. This phenomenon is known as contact instability [9], and is one of the main problems that motivated the development of impedance control. In contrast, Figure 8 demonstrates that the IM-IC successfully controls the robot with negligible effect on its performance.

6 Discussion

Position control and force control are targeted at following a desired trajectory or force profile, respectively, and at minimizing the corresponding trajectory or force error. Impedance control, in contrast, is targeted at attaining the desired impedance, which determines the desired dynamic behavior of the manipulator. Thus, the performance of the impedance control is determined by its ability to attain the desired impedance and to minimize the impedance error.

Direct implementation of impedance control involves changes in the hardware, as in biological systems [31] or special robots [31,32]. However, this requires special hardware whose impedance can be modified on-line. Alternatively, the implementation methods discussed in this paper rely on feedback control to cause the system to respond as having the desired impedance, without actually changing the physical properties of the system. However, the feedback system introduces its own impedance, which may be different from the desired one.

The present paper describes the accuracy/robustness dilemma underlying the two common implementations of feedback based impedance control. The DB-IC may accurately achieve the desired impedance when the dynamics of the system is known, but in addition to its computational complexity, it is not robust to modeling inaccuracies. The PB-IC has been designed to overcome both the control complexity and the lack of robustness, but it introduces impedance inaccuracies. It is noted that the impedance inaccuracy is not related in the quality of the inner-loop position controller but to its dynamic characteristics, which are, in general, different from those of the desired impedance.

The accuracy/robustness dilemma has been demonstrated here using eigenvalue analysis of a one-dimensional system, and simulations of a two-dimensional system. For the sake of simplicity the one-dimensional analysis was conducted for the case when the interaction force is state independent, so the impedance model is decoupled from the controlled manipulator. Eigenvalue analysis indicates that the eigenvalues introduced by the PB-IC differ from the eigenvalues of the desired impendace control, reflecting the impedance accuracy problem. In contrast, sensitivity analysis indicates that the eigenvalues of the DB-IC may shift to the right half plane reflecting the robustness problem.

The case where the interaction force depends on the state of the manipulator is demonstrated in the two-dimensional simulations, in which the manipulator contacts a stiff wall. The interaction force couples the two systems and the overall dynamics is once again determined not only by the desired impedance model but also by the gains of the inner controller. These gains were designed to achieve good position tracking, not to match the desired impedance, and thus the dynamics introduced by the inner controller differs from the desired one. The resulting impendance accuracy problem is demonstrated in the case of a stiffer than expected wall and shown to lead to contact instability.

A novel, practical, and accurate method for impedance control has been proposed, which involves tracking an instantaneous model of the desired impedance (IM-IC). The IM-IC provides a solution to the practical problem of uncertainties in the dynamics

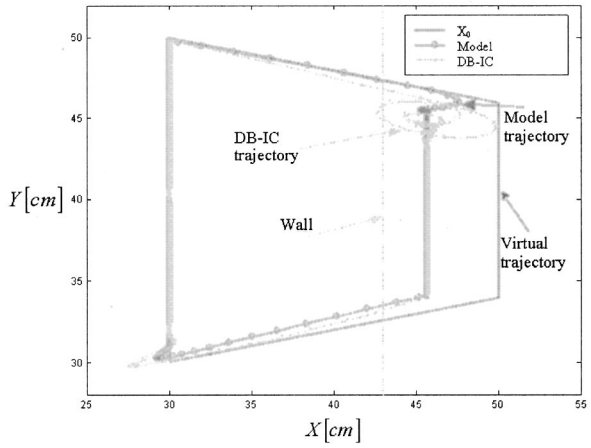

Fig. 7 The DB-IC inadequately controls the robot to perform the task of Fig. 4 with a double than estimated load. The trajectory of the robot with a double than estimated load under the DB-IC (marked with x) significantly deviates from the model trajectory (marked with circles) upon hitting the wall, and the robot temporarily loses contact.

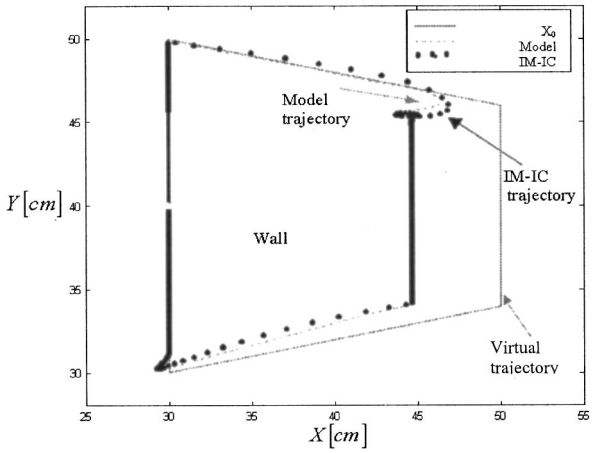

Fig. 8 The IM-IC adequately controls the robot to perform the task of Fig. 4 with double than estimated environment stiffness. The trajectory of the robot under the IM-IC (marked with solid circles) slightly deviates from the model trajectory (dashed line) upon hitting the double-than estimated stiff wall, and the robot maintains contact.

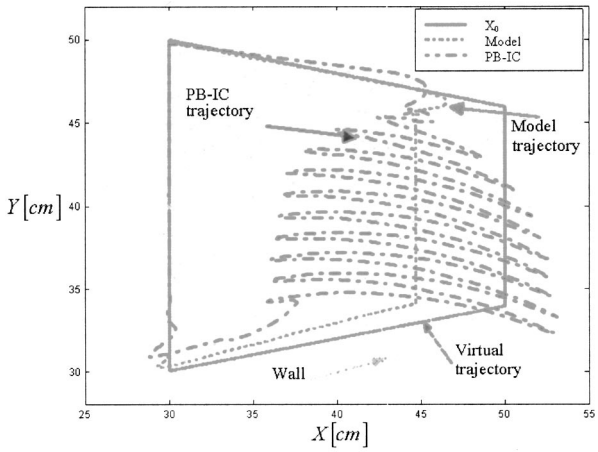

Fig. 9 The PB-IC evokes contact instability when controlling the robot to perform the task of Fig. 4 with a double than estimated environment stiffness. The trajectory of the robot under the PB-IC (dashed-point line) significantly deviates from the model trajectory (dashed line) upon hitting the double than estimated stiff wall, and depicts contact instability.

model of the robot and its environment. A major advantage of IM-IC over PB-IC is the direct correspondence between tracking the instantaneous model and tracking the desired impedance. Proper tuning of the control parameters based on tracking the instantaneous impedance model facilitates impedance tracking. In contrast, tuning the gains of the PB-IC to achieve good trajectory tracking may introduce access stiffness compared to the desired impedance.

The proposed IM-IC tracks the desired impedance well even under modeling uncertainties. This is attributed to the prediction mechanism that considers the robot's actual position. Thus, IM-IC facilitates implementation of impedance control in robots with unknown or poorly specified dynamics models. IM-IC may incorporate a wide variety of inner controllers, which may be tailored by the user for the specific robotic system. Moreover, by tuning the parameters of the inner controller, the user can trade robustness to uncertainties with nominal performance in terms of impedance tracking.

Acknowledgment

This research was supported by the fund for the promotion of research at the Technion.

Appendix: Closed-Loop Description of One-Dimensional Manipulator

The dynamics of the one-dimensional robot is assumed to be described well by Eq. (6) up to parameter uncertainties. The errors in the estimated parameters are defined by

$$\varepsilon_K=\frac{\hat{K}_p-K_p}{K_p};\quad \varepsilon_B=\frac{\hat{B}_p-B_p}{B_p};\quad \varepsilon_M=\frac{\hat{M}_p-M_p}{M_p}, \tag{28}$$

where the $*_p$ parameters denote the actual values and the $\hat{*}_p$ parameters denote the estimated values. Inserting the estimation errors in the control Eqs. (8) and (21) leads to

$$\begin{aligned}U_{DB\text{-}IC}=&-K_p(1+\varepsilon_K)x_p-B_p(1+\varepsilon_B)\dot{x}_p\\&-\frac{M_p(1+\varepsilon_M)}{M_m}[K_m(x_0-x_p)+B_m(\dot{x}_0-\dot{x}_p)-F_{\text{int}}]\\&-F_{\text{int}},\end{aligned} \tag{29}$$

$$\begin{aligned}U_{PB\text{-}IC}=&-K_p(1+\varepsilon_K)x_p-B_p(1+\varepsilon_B)\dot{x}_p-M_p(1+\varepsilon_M)\\&\times[\ddot{x}_m+D_{pb}(\dot{x}_m-\dot{x}_p)+P_{pb}(x_m-x_p)]-F_{\text{int}},\end{aligned} \tag{30}$$

$$\begin{aligned}U_{IM\text{-}IC}=&-K_p(1+\varepsilon_K)x_p-B_p(1+\varepsilon_B)\dot{x}_p-M_p(1+\varepsilon_M)\\&\times[\ddot{x}_{im}+D_{IM}(\dot{x}_{im}-\dot{x}_p)+P_{IM}(x_{im}-x_p)]-F_{\text{int}}.\end{aligned} \tag{31}$$

When the DB-IC described in Sec. 3 is used to control the one-dimensional manipulator described by Eq. (7), it forms a four-dimensional feedback system with a state vector $X=[x_m x_p \dot{x}_m \dot{x}_p]^T$ and an input vector $V=[x_0 \dot{x}_0 F_{\text{int}}]^T$. The closed-loop system can be represented in the state space by $\dot{X}=AX+BV$.

$$A_{DB\text{-}IC}=\begin{bmatrix}0 & 0 & 1 & 0\\ 0 & 0 & 0 & 1\\ -\omega_m^2 & 0 & -2\zeta_m\omega_m & 0\\ 0 & -\omega_m^2(1+\varepsilon_M)+\omega_p^2\varepsilon_K & 0 & -2\zeta_m\omega_m(1+\varepsilon_M)+2\zeta_p\omega_p\varepsilon_B\end{bmatrix}, \tag{32}$$

$$B_{DB\text{-}IC}=\begin{bmatrix}0 & 0 & 0\\ 0 & 0 & 0\\ \omega_m^2 & 2\zeta_m\omega_m & -G_m\\ \omega_m^2(1+\varepsilon_M)+\omega_p^2\varepsilon_K & 2\zeta_m\omega_m(1+\varepsilon_M)+2\zeta_p\omega_p\varepsilon_B & G_p\end{bmatrix}. \tag{33}$$

Similarly, when the PB-IC is used, the state matrices are given by

$$A_{PB\text{-}IC}=\begin{bmatrix}0 & 0 & 1 & 0\\ 0 & 0 & 0 & 1\\ -\omega_m^2 & 0 & -2\zeta_m\omega_m & 0\\ (1+\varepsilon_M)(P-\omega_m^2) & -(1+\varepsilon_M)P+\omega_p^2\varepsilon_K & (1+\varepsilon_M)(D-2\zeta_m\omega_m) & -(1+\varepsilon_M)D+2\zeta_p\omega_p\varepsilon_B\end{bmatrix}, \tag{34}$$

$$B_{PB\text{-}IC}=\begin{bmatrix}0 & 0 & 0\\ 0 & 0 & 0\\ \omega_m^2 & 2\zeta_m\omega_m & -G_m\\ \omega_m^2(1+\varepsilon_M)+\omega_p^2\varepsilon_K & 2\zeta_m\omega_m(1+\varepsilon_M)+2\zeta_p\omega_p\varepsilon_B & G_p\end{bmatrix}. \tag{35}$$

Finally, when the IM-IC described in Sec. 4 is applied, the state matrices are given by

$$A_{IM\text{-}IC}=\begin{bmatrix}0 & 0 & 1 & 0\\ 0 & 0 & 0 & 1\\ -\omega_m^2 & 0 & 2\zeta_m\omega_m & 0\\ 0 & A_{im,42} & 0 & A_{im,41}\end{bmatrix},$$

$$A_{im,42}=-\omega_m^2(1+\varepsilon_M)(dtD_{IM}-2\zeta_m\omega_m dt+1)+\varepsilon_k\omega_p^2, \tag{36}$$

$$\begin{aligned}A_{im,44}=&(1+\varepsilon_M)(dtP_{IM}-2\zeta_m\omega_m dtD_{IM}+4\zeta_m^2\omega_m^2 dt\\&-2\zeta_m\omega_m-dt\omega_m)+2\zeta_p\omega_p\varepsilon_B,\end{aligned}$$

$$B_{IM\text{-}IC}=\begin{bmatrix}0 & 0 & 0\\ 0 & 0 & 0\\ \omega_m^2 & 2\zeta_m\omega_m & -G_m\\ B_{im,31} & B_{im,32} & B_{im,33}\end{bmatrix},$$

$$B_{im,31}=\omega_m^2(1+\varepsilon_M)(dtD_{IM}-2\zeta_m\omega_m dt+1)-\varepsilon_k\omega_p^2, \tag{37}$$

$$B_{im,32}=(1+\varepsilon_M)(2\zeta_m\omega_m dtD_{IM}-4\zeta_m^2\omega_m^2 dt+2\zeta_m\omega_m)$$
$$-2\zeta_p\omega_p\varepsilon_B,$$
$$B_{im,33}=(1+\varepsilon_M)G_m(2\zeta_m\omega_m dt-D_{IM}dt)+G_p.$$

References

[1] Lawrence, D. A., 1988, ''Impedance Control Stability Properties in Common Implementation,'' Proceedings of the IEEE International Conference on Robotics and Automation, pp. 1185–1190.

[2] Lu, W. S., and Meng, Q. H., 1991, ''Impedance Control With Adaptation for Robotic Manipulations,'' IEEE Trans. Rob. Autom., **7**, pp. 408–415.

[3] Surdilovic, D., and Kirchhof, J., 1996, ''A New Position Based Force/Impedance Control for Industrial Robots,'' Proceedings of the IEEE International Conference on Robotics and Automation, Minneapolis.

[4] Pelletier, M., and Doyon, M., 1994, ''On the Implementation and Performance of Impedance Control on Position Controlled Robots,'' Proceedings of the IEEE Conference on Robotics and Automation, pp. 1228–1233.

[5] Guliaume, M., Ezio, M., and Sylvie, B., 1998, ''Impedance Based Combination of Visual and Force Control,'' Proceedings of the 1998 IEEE International Conference on Robotics & Automation, Leuven, Belgium.

[6] Hsia, T. C., Lasky, T. A., and Guo, Z., 1991, ''Robust Independent Joint Controller Design for Industrial Robot Manipulators,'' IEEE Trans. Ind. Electron., **38**(1), pp. 21–25.

[7] Hogan, N., 1985, ''Impedance Control: An Approach to Manipulation,'' J. Dyn. Syst., Meas., Control, **107**, pp. 1–24.

[8] Hogan, N., 1987, ''Stable Execution of Contact Tasks Using Impedance Control,'' in Proceedings of the IEEE International Conference on Robotics and Automation, Raleigh, NC, pp. 1047–1054.

[9] Colgate, J. E., and Hogan, N., 1989, ''An Analysis of Contact Instability in Terms of Passive Physical Equivalents,'' in Proceedings of the IEEE International Conference on Robotics and Automation, pp. 404–409.

[10] Bonitz, R. G., and Hsia, T. C., 1996, ''Internal Force-Based Impedance Control for Cooperating Manipulators,'' IEEE Trans. Rob. Autom., **12**, pp. 78–79.

[11] Ikeura, R., and Inooka, H., 1995, ''Variable Impedance Control of a Robot for Cooperation With a Human,'' Proceedings of the IEEE International Conference on Robotics and Automation.

[12] Kao, I., and Cutkosky, R. M., 1997, ''Robotic Stiffness Control and Calibration as Applied on Human Grasping Tasks,'' IEEE Trans. Rob. Autom., **13**, pp. 557–566.

[13] Newman, S. W., Branicky, S. M., and Poddgurski, A. H., 1999, ''Force-Responsive Robotic Assembly of Transmission Components,'' Proceedings of the 1999 IEEE International Conference on Robotics and Automation, pp. 2096–2102.

[14] Surdilovic, D., 1996, ''Contact Stability Issues in Position Based Impedance Control: Theory and Experiments,'' Proceedings of the IEEE International Conference on Robotics and Automation, Minneapolis.

[15] Chan, S. P., and Liaw, H. C., 1996, ''Generalized Impedance Control of Robot for Assembly Tasks Requiring Compliant Manipulation,'' IEEE Trans. Ind. Electron., **43**, pp. 453–461.

[16] Newman, W. S., Branicky, M., and Pao, Yoh-Han, 2001, ''Intelligent Strategies for Compliant Robotic Assembly,'' Proceedings of the 2001 IEEE International Conference on Robotics and Automation.

[17] Siciliano, B., and Villani, L., 1999, *Robot Force Control*, Kluwer Academic Publishers, Norwell, Massachusetts, USA.

[18] Chan, C. C., and Danwei, W., 1994, ''Learning Impedance Control For Robotic Manipulation,'' The Third International Conference on Automation, Robotics and Computer Vision, Nanyang Technol. Univ. Singapore, Vol. 3.

[19] Colbaugh, R., Seraji, H., and Glass, K., 1993, ''Direct Adaptive Impedance Control of Robot Manipulators,'' J. Rob. Syst., **10**, pp. 217–248.

[20] Jung, S., Hsia, T. C., and Bonitz, R. G., 1997, ''On Robust Impedance Force Control of Robot Manipulators,'' Proceedings of the IEEE International Conference on Robotics and Automation, Piscataway, NJ, Vol. 3, pp. 2057–2062.

[21] Lasky, T. A., and Hsia, T. C., 1991, ''On Force-Tracking Impedance Control of Robot Manipulators,'' in Proceedings of the IEEE International Conference on Robotics and Automation, Sacramento, CA, pp. 274–280.

[22] Salisbury, J. K., 1980, ''Active Stiffness Control of a Manipulator in Cartesian Coordinates,'' Proceedings of the IEEE Decision and Control Conference, Albuquerque, NM.

[23] Newman, W. S., 1992, ''Stability and Performance Limits of Interaction Controllers,'' ASME J. Dyn. Syst., Meas., Control, **114**, pp. 563–570.

[24] Glosser, G. D., and Newman, W. S., 1994, ''Implementation of a Natural Admittance Controller on an Industrial Manipulator,'' Proceedings of the IEEE International Conference on Robotics and Automation, pp. 1209–1215.

[25] Heinrichs, B., and Sepehri, N., 1999, ''A Limitation of Position Based Impedance Control in Static Force Regulation: Theory and Experiments,'' Proceedings of the IEEE International Conference on Robotics and Automation, Detroit, Michigan.

[26] Whitney, D. E., 1977, ''Force Feedback Control of Manipulator Fine Motion,'' ASME J. Dyn. Syst., Meas., Control, **99**, pp. 91–97.

[27] Valency, T., 1999, ''Instantaneous Model Impedance Control for Robots,'' M.Sc. thesis, Technion-Israel Institute of Technology, Haifa, Israel.

[28] Valency, T., and Zacksenhouse, M., 2000, ''Instantaneous Model Impedance Control for Robots,'' Proceeding of the IEEE/RSJ International Conference on Intelligent Robots and Systems, November 2000, Kagawa University, Takamatsu, Japan.

[29] Katsuhiko, O., 1970, *Modern Control Engineering*, Prentice-Hall, Englewood Cliffs, NJ.

[30] Surdilovic, D., 1998, ''Synthesis of Impedance Control Laws at Higher Control Levels: Algorithms and Experiments,'' Proceedings of the IEEE International Conference on Robotics and Automation, Leuven, Belgium.

[31] Hogan, N., 1984, ''Adaptive Control of Mechanical Impedance by Coactivation of Antagonist Muscles,'' IEEE Trans. Autom. Control, **AC-29**, pp. 681–690.

[32] Williamson, M. M., 1998, ''Neural Control of Rhythmic Arm Movements,'' IEEE Trans. Neural Netw., **11**, pp. 1379–1394.